



The influence of yttrium addition on the GFA of selected iron-based BMG

W. Pilarczyk ^{a,*}, A. Mucha ^b

^a Division of Nanocrystalline and Functional Materials and Sustainable Pro-ecological Technologies, Institute of Engineering Materials and Biomaterials, Silesian University of Technology, ul. Konarskiego 18a, 44-100 Gliwice, Poland

^b Division of Materials Processing Technology, Management and Computer Techniques in Materials Science, Institute of Engineering Materials and Biomaterials, Silesian University of Technology, ul. Konarskiego 18a, 44-100 Gliwice, Poland

* Corresponding author: E-mail address: wirginia.pilarczyk@polsl.pl

Received 25.05.2010; published in revised form 01.08.2010

ABSTRACT

Purpose: The main aims of this work is the presentation of the influence of yttrium addition on the structure and properties of BMG and the production attempt of chosen Fe-based bulk metallic alloys.

Design/methodology/approach: The studies were carried out on Fe-based alloys ingots with the following compositions $\text{Fe}_{43}\text{Co}_7\text{Cr}_{15}\text{Mo}_{14}\text{C}_{15}\text{B}_6$, $\text{Fe}_{41}\text{Co}_7\text{Cr}_{15}\text{Mo}_{14}\text{C}_{15}\text{B}_6\text{Y}_2$ and $\text{Fe}_{39}\text{Co}_7\text{Cr}_{15}\text{Mo}_{14}\text{C}_{15}\text{B}_6\text{Y}_4$. Samples were prepared by induction melting of the pure Fe, Co, Cr, Mo, C, B and Y elements in argon atmosphere. The structure was tested with X-ray diffraction. In order to investigate the structure scanning electron microscopy was used. The thermal properties of the alloys were examined by DTA and DSC methods.

Findings: Bulk metallic glasses with yttrium addition exhibit high glass forming ability. These materials depending on accurate chemical composition present excellent corrosion resistance, magnetic, electric and mechanical properties. Fe-based materials with yttrium addition are potential materials for industrial applications.

Research limitations/implications: It is very difficult to obtain a metallic glass of $\text{Fe}_{43}\text{Co}_7\text{Cr}_{15}\text{Mo}_{14}\text{C}_{15}\text{B}_6$, $\text{Fe}_{41}\text{Co}_7\text{Cr}_{15}\text{Mo}_{14}\text{C}_{15}\text{B}_6\text{Y}_2$ and $\text{Fe}_{39}\text{Co}_7\text{Cr}_{15}\text{Mo}_{14}\text{C}_{15}\text{B}_6\text{Y}_4$ alloys. All tested alloys have crystalline structure. Taking into account all the factors affecting the test samples, we can conclude that the received samples have not an amorphous structure for the non-uniform distribution of yttrium in materials.

Originality/value: Overall presentation of the yttrium addition influence, the formation and the study of Fe-Co-Cr-Mo-C-B-Y bulk metallic materials.

Keywords: Amorphous materials; Bulk Metallic Glasses; Fe-based alloys; Yttrium addition

Reference to this paper should be given in the following way:

W. Pilarczyk, A. Mucha, The influence of yttrium addition on the GFA of selected iron-based BMG, Archives of Materials Science and Engineering 44/2 (2010) 87-95.

MATERIALS

1. Introduction

The large rare earth (RE) elements, such as yttrium, scandium, gadolinium, erbium even in small addition have been

shown to be advantageous in bulk glass formation [1]. The RE elements have similar atomic size, physical and chemical properties. Therefore, proper addition of different RE elements should have the influence on the glass forming ability (GFA) of the bulk metallic glasses-forming (BMG) alloys.

The RE elements are the important minor addition materials which have an important impact on the glass production. Since the beginning of the BMG development, RE elements have been used as the BMG-forming base and the minor alloying additions [2]. They have a serious effect on the manufacturability of some BMGs, which depends on preparation and processing conditions such as vacuum and impurity of environment. Oxygen or other impurities would significantly reduce the GFA.

F. Guo, S.J. Poon et al. [1] maintain that family of yttrium metallic alloys is able to form glassy ingots directly from the liquid or to form glassy rods with diameters over 20 mm.

Yttrium is one of the addition elements for improving (GFA) and producing of BMG-forming alloys [1]. Proper Y addition ($1 < Y < 6 \text{ at.}\%$) can considerably improve the GFA of the Zr-based alloy by suppressing the precipitation of the Zr_2Ni Laves phase. Wang et al. have studied $(\text{Zr}_{55}\text{Al}_{15}\text{Ni}_{10}\text{Cu}_{20})_{100-x}\text{Y}_x$ where $x=0, 0.5, 1, 2, 4, 6 \text{ at.}\%$. The as-cast samples in rod form with diameter of 5 mm contain a Laves phase. The addition of 0.5 at% Y suppresses the precipitation of the Zr_2Ni phase but induces AlNiY crystalline phase. This phase is induced in the glassy matrix. With the increase of Y addition up to 2 at.% the X-ray diffraction patterns of crystalline AlNiY phase become lower and wider. When the addition is 4 at.% no crystalline peaks were observed. Further addition of Y leads again to the precipitation of crystalline phase. No exothermic peaks were observed for the alloy without Y. The 0.5 at.% Y addition causes the formation of amorphous phase, an exothermic peak was observed on DTA curve. The DTA curves of the alloys with 2-4 at.% Y addition exhibit sharp exothermic peaks. It has been stated that the large fraction of amorphous phase was formed in produced alloys. These results indicate that a proper Y addition can suppress Laves phase formation and improve the GFA of Zr-Al-Ni-Cu system alloy.

E.S. Park and D.H. Kim [3] have been investigating enhancement of plasticity and the occurrence of liquid state phase separation by substituting Zr with Y in $\text{Cu}_{46}\text{Zr}_{47-x}\text{Y}_x\text{Al}_7$ ($x = 0, 2, 5, 10, 15, 20, 25, 30, 35$) alloys. Since Y has a positive enthalpy of mixing with Zr (+35 kJ/mol) in the liquid state, the alloy composition moves to the metastable miscibility gap of the two amorphous phases with increasing Y content. The study shows that phase separation into Y-rich and Zr-rich amorphous phases occurs during cooling from the liquid state when the Y content is above 15 at.%. There is the opinion [3] that the bulk amorphous alloys consisting of two phase-separated amorphous phases exhibit extreme brittleness, while the single-phase amorphous alloys containing 2-5 at.% of Y exhibit enhanced plasticity because of the chemical inhomogeneity in the amorphous matrix. The results indicate that the addition of an element having a positive enthalpy of mixing with the constitutive element in bulk amorphous alloys can increase the plasticity as well as the glass-forming ability, but for a limited composition range.

Yttrium addition can improve the GFA of Fe-based BMGs, too [2,4,5]. Even 2 at.% Y in Fe-based alloys greatly enlarged their attainable maximum sizes. The yttrium is able to scavenge oxygen from the undercooled liquid and lower the liquidus temperature in Fe-based alloys.

Yttrium plays the empirical roles to obtain high GFA for the Fe-Nb-B-Si system [2]. The atomic radius of Y is 0.178 nm, which is larger than 0.126 nm of Fe, 0.146 nm of Nb, 0.098 nm of B and 0.132 nm of Si. The heat of mixing in the Fe-Y, B-Y, Si-Y

binary system is -1, -35, and -56 kJ/mol, respectively. The scientists J.M. Park et al. [4] conducted research in the Fe-Nb-B-Si system. They have investigated the effect of yttrium on the GFA of $(\text{Fe}_{72}\text{Nb}_4\text{B}_{20}\text{Si}_4)_{100-x}\text{Y}_x$ ($x=0-5$) alloys. As a result of the tests it was observed that the amorphous phase occurred in all rapidly solidified ribbons and rods with diameters of 4-5 mm. All DSC curves exhibited one endothermic peak, which is characteristic of the glass transition to undercooled liquid, followed by exothermic peaks corresponding to the crystallization of the undercooled liquid. In the opinion of the authors of this publication the $(\text{Fe}_{72}\text{Nb}_4\text{B}_{20}\text{Si}_4)_{97}\text{Y}_3$ alloy shows the highest GFA among the investigated alloys, enabling formation of maximum 4 mm diameter glassy rods [4].

In the last years, the development of Fe-based BMGs with higher GFA in conjunction with high strength has been required [5,6,7]. Recently, Fe-based BMGs with critical diameters up to 12 mm have been formed in Fe-(Cr, Mo, Mn)-(C, B)-Y system through the additional effect of small amounts of Y on the bulk glassy Fe-(Cr, Mo)-(C, B) alloys [8]. These alloys exhibit poor mechanical properties because of their extremely brittle nature. Therefore, there is the need for more investigations in this field.

K. Amiya and A. Inoue have found that Fe-(Cr,Mo)-(C,B)-Tm BMGs exhibit simultaneously high strength above 4000 MPa as well as high GFA with critical diameter of over 10 mm. They have been the investigated alloys with RE elements. The achievement of high strength and high GFA indicates the possibility of applying the Fe-(Cr,Mo)-(C,B)-Tm glassy alloys to various engineering materials [8].

On the basis of the investigations into the relationship between yttrium containing and corrosion resistance [9,10], Wang et al. confirmed the previous test results [9]. In earlier investigations it was noted that minor addition of yttrium to amorphous alloy can improve the GFA, corrosion resistance and brittle-plastic transition [9]. For the test, the authors used $\text{Fe}_{50-x}\text{Cr}_{15}\text{Mo}_{14}\text{C}_{15}\text{B}_6\text{Y}_x$ alloy ingots ($x=0, 0.5, 1, 1.5, 2 \text{ at.}\%$). Yttrium-free rods with diameter of 1 mm and alloys in rod form with diameter of 2 mm were prepared by suction casting of the molten alloys into a copper mold. It has been shown that other yttrium-free and yttrium-containing samples possess a fully glassy structure. The scientists present cation (yttrium) doping controlled stabilization of passive films in corrosion of obtained bulk amorphous alloys. As it was expected, yttrium cation doping can greatly influence the generation of oxygen vacancies and the diffusion of oxygen through the oxide films. As a result of the tests it was noted that the deviation of dependence of corrosion resistance on donor density at high Y addition alloys is in relation to the changes in composition and thickness of passive films [9]. The workers confirmed that the Y addition induces changes in composition and thickness of passive film. Therefore, it has beneficial effects on corrosion, which has been seen from electrochemical measurements. From the analysis of this article data it can be concluded that the corrosion resistance is very sensitive to minor yttrium alloying, ascribed to yttrium doping induced structural changes in the passive films.

Ponnambalam et al. have successfully developed new alloy composition in Fe-Co-Cr-Mo-C-B-Y, Fe-Cr-Co-Mn-Mo-C-B-Y and Fe-Cr-Mo-C-B-Er alloy systems, which allow to produce of BMGs with the maximum sizes of up to 16 mm and 12 mm in diameters, respectively. Fe-based bulk amorphous rods of 3 mm

in diameter and a composition of $\text{Fe}_{41}\text{Cr}_{15}\text{Mo}_{14}\text{C}_{15}\text{B}_6\text{Y}_2\text{Co}_7$ were produced by copper mold casting [11]. The XRD pattern of as-cast sample exhibit a broad diffraction peak without any sharp peaks, indicating that the structure of obtained 3 mm in diameter rods are fully amorphous. These rods contain pores (about 2 %). To get rid of the pores, samples were hot isostatically pressed (HIP-Hot Isostatic Pressing) at 863 K. This temperature is in the supercooled liquid temperature range between the glass transition temperature and the crystallization temperature of tested alloy, under the pressure of 200 MPa. It has been shown that HIP results in an increase of the density of the samples from 7.9 g/cm^3 to 8.0 g/cm^3 , decrease of the porosity from 2% to 1%, and creating a little of fraction of unknown crystalline phase. This is because the pressure and thermal effects of HIP induce structure relaxation which leads to partial crystallization of the amorphous phase. The HIP process did not lead to any improvement in mechanical properties of obtained bulk glassy alloy. On the basis of the investigation, the authors concluded that the partial devitrification which occurs during HIP process is mainly due to the thermal effect rather than the used pressure effect.

As mentioned above, Fe-based BMG with yttrium addition, which are the basis of excellent soft magnetic properties materials, are of special importance. These alloys called the scientists' attention to their high glass forming ability, magnetic and mechanical properties [12].

Guo and co-workers [12] have produced $\text{Fe}_{70-x}\text{Co}_x\text{Hf}_5\text{Mo}_7\text{B}_{15}\text{Y}_3$ 3 mm fully amorphous rods. The effect of Co substitution for Fe on the GFA and magnetic properties has been investigated in this work. The constituent elements in Fe-Co-Hf-Mo-B-Y system can be sorted into five groups, i.e. (Fe, Co), Hf, Mo, B, Y, according to their positions in periodical table. The authors [12] suppose that the addition of a suitable amount of Co (4-12 at. %) would lead to a more sequential change in the atomic size in the order of $\text{Y} > \text{Hf} > \text{Mo} > \text{Co} > \text{Fe} > \text{B}$. Furthermore, the enthalpies of mixing are -35 kJ/mol for the Co-Hf pair, -5 kJ/mol for the Co-Mo pair, -22 kJ/mol for the Co-Y pair, they are larger than those for Fe-Hf (-21 kJ/mol), Fe-Mo (-2 kJ/mol) and Fe-Y (-1 kJ/mol), adequately. This phenomenon can suggest that the above factors would result in denser topological package of atoms and hinder one another from crystallization process, as a result, enhance the stability and increase the GFA. As a result of the tests it was observed that the $\text{Fe}_{70-x}\text{Co}_x\text{Hf}_5\text{Mo}_7\text{B}_{15}\text{Y}_3$ amorphous alloys exhibit a large supercooled liquid region (exceeding 50 K) and high glass transition temperature (exceeding 870 K), proving a high thermal stability. What is more, the substitution of Co for Fe improves soft magnetic properties of the obtained Fe-based BMGs. The high saturation magnetization with a very low coercivity of the novel BMG alloys with Y addition exhibit promising application in magnetic industry [12].

C.Y. Lin and T.S. Chin [13] have conducted investigation of ternary Fe-Y-B system alloy and Fe-(Co,Ni)-Y-B quaternary bulk metallic glasses. The ribbons and rods with nominal compositions $\text{Fe}_{78-x}\text{Y}_x\text{B}_{22}$ ($x=4, 5, 6, 7, 8, 9$), $\text{Fe}_{72-y}\text{Co}_y\text{Y}_6\text{B}_{22}$ ($y=0, 10, 20, 30, 36, 50$) and $\text{Fe}_{72-z}\text{Ni}_z\text{Y}_6\text{B}_{22}$ ($z=5, 10, 15, 20$) were prepared. The GFA, thermal and magnetic properties were studied. In $\text{Fe}_{78-x}\text{Y}_x\text{B}_{22}$ alloys, the glass transition temperature (T_g) and crystallization temperature (T_x) gradually increases with Y content from 843 K to 928 K and 887 K to 986 K, adequately. The melting point ($T_m \sim 1400$ K) and liquidus temperature

($T_l \sim 1425$ K) remain nearly unchanged with Y content. The supercooled liquid region ($\Delta T_x = T_x - T_g$) gradually increases with Y content, reaches the maximum value 80 K for $x=7$ and $x=8$ and then decreases. The reduced glass transition temperature and γ factor increase with Y content. From the analysis of obtained data it can be concluded that the $\text{Fe}_{72}\text{Y}_6\text{B}_{22}$ ($x=6$) has the best GFA which is able to form a bulk glassy rod at least 2 mm in diameter among all studied ternary Fe-Y-B alloys [13]. It wasn't expected because the $\text{Fe}_{72}\text{Y}_6\text{B}_{22}$ alloy exhibits neither the largest ΔT_x nor the largest T_{rg} and not the largest γ value of the $\text{Fe}_{78-x}\text{Y}_x\text{B}_{22}$ system alloy. From the analysis of literature data good glass former is in deep eutectic systems. In the Fe-Y-B system good glass formers locate in ternary eutectic region of Fe, Fe_2B and $\text{Fe}_4\text{B}_4\text{Y}$. Ultimately, it can be noted that the thermal criteria value of ternary Fe-Y-B amorphous alloys are rather high compared with other kind of Fe-based BMGs with similar diameters. The results of Lin group and Zhang group overlap. They have examined that ΔT_x was 72 K for $\text{Fe}_{70.2}\text{Y}_{5.8}\text{B}_{24}$ alloy and the T_{rg} was 0.57 for $\text{Fe}_{75.7}\text{Y}_{4.3}\text{B}_{20}$ [13].

On the basis of the investigations into the relationship between ternary and quaternary BMG Lin et al. confirmed the previous tests and perfected them. Their tests showed that quaternary BMGs are possible when the replacement of Fe by Co is not higher than 36 at.%, or Ni replacement is not higher than 10 at. %. In the described experiments excellent magnetic, electric and thermal properties were obtained. These (Fe,Co,Ni)-Y-B BMGs are potential materials for industrial applications, for example such as cores for power transformers [13].

The scientists X.H. Tan et al. [14] have conducted research in the Fe-Co-Nd-Y-B magnet prepared by suction casting. They have made an attempt to improve the GFA and magnetic properties of the bulk Fe-Co-Nd-B alloy by addition of yttrium. The test results show that the crystalline peaks can be seen for this alloy without the addition of yttrium. The diffraction patterns show the peaks characteristic for α -Fe, CoB and $\text{Fe}_{77.2}\text{Nd}_{22.8}$ phase. For the $\text{Fe}_{65}\text{Co}_{10}\text{Nd}_3\text{Y}_2\text{B}_{20}$ sample, α -Fe and $\text{Fe}_{77.2}\text{Nd}_{22.8}$ phases were presented with amorphous phases. Broad peak with small crystalline peaks of α -Fe and Fe_2Y can be seen for alloy with 6 at.% Y. What is more, with a further increase in Y content to 10 at.%, sharp crystalline peaks have been formed. In this work it was observed that the optimum content of Y in Fe-Co-Nd-Y-B system alloy is around 6 at.% and the experiments confirmed that a small addition of Y is very effective in improving the GFA of these alloys, but more than 6 at.% of Y addition would lead to the precipitation of Fe_2Y phase, which would deteriorate GFA of the alloy. The X-ray diffraction results have been confirmed by differential thermal analysis. It is indicated that the sample contains a certain amount of amorphous phase. The as-cast $\text{Fe}_{61}\text{Co}_{10}\text{Nd}_3\text{Y}_6\text{B}_{20}$ alloy presented good soft magnetic properties. However, the alloy showed hard magnetic properties after annealing at 948 K for 30 min. In the authors assumption this approach can provide one promising way for the production of bulk magnets by the simple process of copper mold casting and subsequent heat treatment. To sum up, it can be concluded that Y addition improves GFA, what has to be understood in three aspects [14]:

- Y has a stronger affinity with the oxygen, resulting in the formation of yttrium oxide that can alleviate the harmful effect of oxygen,

- Y satisfies the three rules for achievement of large glass forming ability formulated by Inoue,
- Y addition can adjust the compositions closer to the eutectic and thus enhance stability of the liquid phase.

In accordance with earlier publications, H.W. Chang [15] has followed the rules which were established by C.Y. Lin and his co-workers. They created simple rules of composition selection for Fe-B bulk glassy alloys by modifying the Inoue's empirical rules:

- M is an element with an atomic radius at least 130% that of Fe,
- M possesses eutectic points with both Fe and B,
- M-Fe eutectic is at the Fe-rich.

Among the $M_6Fe_{72}B_{22}$ based ternary system alloys, the BMG with larger diameter of 2 mm could be achieved for the alloys with $M=Y, Sc, Dy, Er$. As a result of the laboratory tests, the $Y_6Fe_{72}B_{22}$ alloy shows the highest saturation magnetization and great potential for application due to the reasonable price and available yttrium [15].

Chang et al. [15] have produced $Y_{6-x}Fe_{72}B_{22}Ti_x$, $Y_6Fe_{72-x}B_{22}Ti_x$, $Y_6Fe_{72}B_{22-x}Ti_x$, ($x=0, 2$ and 4) alloys in rod form with various diameters of 2, 3, 4 mm and 20 mm in length by injection casting into a copper mold. The tests reveal that insufficient Y content could degrade the GFA of alloy in Y-Fe-B-Ti system, 4 at.% Y seems to be the minimum value to keep its high GFA. The substitution 2 at.% Ti for Y in $Y_6Fe_{72}B_{22}$ alloys not only make the bulk glassy rod as large as 3 mm in diameter, but also result in superior soft magnetic properties. The Curie temperature is decreased slightly when a small amount of Y is substituted by Ti. The thermal evidence from this work prove that the alloys with larger supercooled liquid region have better GFA to obtain the BMG rod with larger diameter. The reduced glass transition temperature is decreased with Ti content due to the decrease of glass transition temperature. In author's opinion, the difference in the supercooled liquid region seems to be proper to explain the increase in GFA by substituting 2 at.% Ti for Y [15].

The substituting 2 and 4 at.% Ti for Fe in $Y_6Fe_{72}B_{22}$ alloys decreased the saturation magnetization and Curie temperature due to the decrease in the amount of magnetic element Fe. Besides, the GFA is deteriorated with the substitutions of Ti for B in Y-Fe-B-Ti system.

M. Regev et al. [16] have investigated the influence of the cooling rate on bulk metallic glass formation in significant difference yttrium concentration alloys: $Mg_{80}Cu_{15}Y_5$ and $Mg_{80}Cu_{10}Y_{10}$. It has been shown that only pattern obtained from the $Mg_{80}Cu_{15}Y_5$ melt spun specimen may be characterized as an amorphous one and to some extent, the $Mg_{80}Cu_{10}Y_{10}$ molten one. It is only necessary to mention that Mg and Mg_2Cu peaks were identified in all cases whereas no reflections of free Y were detected. This is probably possibly due to its small volume fraction. However, Mg and Mg_2Cu reflections are slightly shifted to lower angles (higher d-spacings), possibly due to the existence of dissolved Y [16]. It was found that $Mg_{80}Cu_{10}Y_{10}$ was completely crystalline. In the opinion of the authors of this publication, taking into consideration the fact that the Y does not or almost does not dissolve in the alloy, proves that chemical composition calculations should be based on the Mg and Cu content without taking the Y into account [16].

Yttrium addition can improve the GFA of Cu-based BMG, too [1,17,18,19]. A little yttrium addition (1-2 at.%) can

significantly improve the manufacturability of Cu-Zr-Al alloys through the suppression of the growth of eutectic clusters and the precipitation of the primary dendrite phase.

2. Experimental procedure

The aim of the presented work is the manufacturing, examine the structure and properties $Fe_{43}Co_7Cr_{15}Mo_{14}C_{15}B_6$, $Fe_{41}Co_7Cr_{15}Mo_{14}C_{15}B_6Y_2$ and $Fe_{39}Co_7Cr_{15}Mo_{14}C_{15}B_6Y_4$ bulk metallic alloys and define the influence of yttrium addition using XRD, SEM, DTA and DSC methods.

Fe-based alloys ingots with follow compositions (Tables 1-3) of $Fe_{43}Co_7Cr_{15}Mo_{14}C_{15}B_6$, $Fe_{41}Co_7Cr_{15}Mo_{14}C_{15}B_6Y_2$ and $Fe_{39}Co_7Cr_{15}Mo_{14}C_{15}B_6Y_4$ where prepared by induction melting of the pure Fe, Co, Cr, Mo, C, B and Y elements in argon atmosphere. Each of them was melted double. In this case used pressure die casting method. The master alloy was melted in a quartz crucible using an induction coil and pushed thereafter in a copper mould by applying an ejection pressure. The samples was cast with diameters of $\phi=1.5$ mm and $\phi=2$ mm.

Table 1.

Chemical composition of $Fe_{43}Co_7Cr_{15}Mo_{14}C_{15}B_6$ alloy

No	Elements	at. [%]	mass. [%]	mass. per 30g.
1	Fe	43	46.34	13.90
2	Co	7	7.96	2.38
3	Cr	15	15.05	4.51
4	Mo	14	25.91	7.58
5	C	15	3.47	1.04
6	B	6	1.25	0.37

Table 2.

Chemical composition of $Fe_{41}Co_7Cr_{15}Mo_{14}C_{15}B_6Y_2$ alloy

No	Elements	at. [%]	mass. [%]	mass. per 30g.
1	Fe	41	43.62	13.08
2	Co	7	1.86	0.55
3	Cr	15	14.86	4.45
4	Mo	14	25.59	7.67
5	C	15	3.43	1.02
6	B	6	1.23	0.37
7	Y	2	3.38	1.01

Table 3.

Chemical composition of $Fe_{39}Co_7Cr_{15}Mo_{14}C_{15}B_6Y_4$ alloy

No	Elements	at. [%]	mass. [%]	mass. per 30g.
1	Fe	42.40	39	12.72
2	Co	8.03	7	2.40
3	Cr	15.18	15	4.55
4	Mo	26.14	14	7.84
5	C	3.50	15	1.05
6	B	1.26	6	0.37
7	Y	3.46	4	1.03

Glassy and crystalline structure were tested with X-ray diffraction (XRD) using a Seifert - FPM XRD 7 diffractometer with Co K α radiation at 35 kV. The data of diffraction lines were recorded by means of the stepwise method within the angular range of 20° to 100° and the counting time in the measuring point was 3 s.

Using differential scanning calorimetry (DSC) it is possible to observe mix and crystallization events as well as glass transition temperatures T_g. The thermal stability associated with glass transition temperature, supercooled liquid and crystallization temperature was investigated by DSC methods using DSC822 Mettler Toledo and differential thermal analysis at a constant heating rate of 50 K/min.

Scanning electron microscope (SEM) by a large depth of view allows to observe the surface elements. It is a primary tool for measuring and research which is used to analyze the morphology fracture condition and evaluate its morphology. The microscopic observation of the morphology of studied materials with different diameter was carried out by means of the OPTON DS 940 scanning electron microscope, within the magnification 100-1000 times.

3. Results

3.1. X-ray diffraction results

X-ray studies were performed to determine the structure of the analysed alloys. Figs from 1 to 3 shows represent the sets of X-ray diffraction which have been received for the surface of the Fe₄₃Co₇Cr₁₅Mo₁₄C₁₅B₆, Fe₄₁Co₇Cr₁₅Mo₁₄C₁₅B₆Y₂ and Fe₃₉Co₇Cr₁₅Mo₁₄C₁₅B₆Y₄ cast rods.

Unfortunately, the structure of amorphous alloys has not been obtained. All samples which were tested immediately after the casting exhibit the crystalline structure. This means that atoms exhibit long-range ordering. On the diffractograms it show that there are no spectrum which is characterized by an amorphous structure. Instead we can observe clear, sharp peaks, which characterize the crystal structure. X-ray qualitative phase analysis showed that the phase composition of analysed samples with 1.5 mm and 2 mm diameters is as follows: in the sample which does not containing yttrium there are metallic phases on the iron matrix α (ferrite) and γ (austenite). There are much more austenitic phases which is confirmed by the intensity of the diffraction lines. The reason for this fact is probably the high content of cobalt in the melt, which caused its austenitizing. The actual composition of the γ phase, probably would better show the pattern γ -(Fe, Cr, Co). There are, moreover carbides and boron carbides. There is most of all carbide with Cr₂₆C₆ phase. This is most likely Fe₂₃(C,B)₆ compound. There is also cementite Fe₃C and Co₂C. Below Table 4 shows the catalog numbers JCPDS-ICDD detected compounds and their determination in the diffractograms.

Figure 1 show the results of X-ray diffraction a Fe₄₃Co₇Cr₁₅Mo₁₄C₁₅B₆ alloy which was obtained by casting in the form of a rod with the 1.5 mm and 2 mm diameter. The X-ray diffraction shows that the dominant phase in the alloy is

Fe₂₃(C,B)₆. In addition, there is also phase α -Fe, γ -Fe, Fe₃C and Co₂C. The increase of the background and broadening of diffraction lines on the diffractograms cannot be observed.

Table 4.

The identified phases, catalog number and their mark on the diffractograms [20]

No	Phase	Catalog number	Phase marking
1	α -Fe	6-696	▲
2	γ -Fe	31-619	◆
3	Cr ₂₆ C ₆	35-783	-
4	Fe ₂₃ (C,B) ₆	12-570	●
5	Fe ₃ C	35-772	■
6	Co ₂ C	5-704	▬
7	(Fe,Cr) ₇ C ₃	5-720	○
8	FeB	3-937	▬
9	Co ₆ W ₆ C	23-939	■

Comparing the results of analysed Fe₄₃Co₇Cr₁₅Mo₁₄C₁₅B₆ alloy with 1.5 mm and 2 mm diameter, it can be observed that increasing a diameter of the analysed sample slightly increases the intensity of the peaks - they increase or decrease.

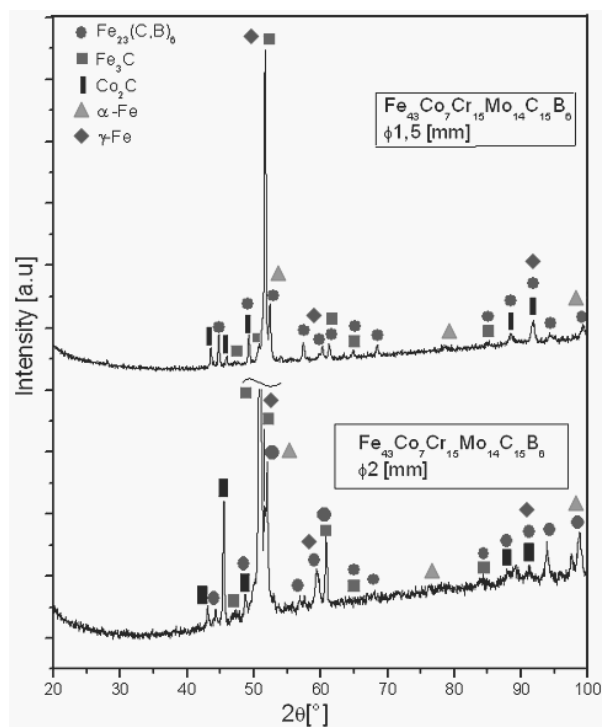


Fig. 1. X-ray diffraction patterns of the Fe₄₃Co₇Cr₁₅Mo₁₄C₁₅B₆ alloys rods with diameters of 1.5 mm and 2 mm

The following diffraction patterns show the results of X-ray analysis for the rods with the chemical composition of $\text{Fe}_{41}\text{Co}_7\text{Cr}_{15}\text{Mo}_{14}\text{C}_{15}\text{B}_6\text{Y}_2$ and $\text{Fe}_{39}\text{Co}_7\text{Cr}_{15}\text{Mo}_{14}\text{C}_{15}\text{B}_6\text{Y}_4$. The analysed samples have the yttrium in their chemical composition. Yttrium is a chemical element that had a significant impact on the structure of the samples. Yttrium was added to increase the GFA and to improve properties of the alloy. The following graphs show that with an increase in the diameter of the sample the intensity of the peaks increases. There is an increase of the background and the broadening of diffraction lines on the graph may be connected with the formation of amorphous phase (Fig. 2).

The following X-ray diffraction (Fig. 2) presents a summary of the results of X-ray phase analysis for the $\text{Fe}_{41}\text{Co}_7\text{Cr}_{15}\text{Mo}_{14}\text{C}_{15}\text{B}_6\text{Y}_2$ alloy rods with 1.5 mm and 2 mm diameters.

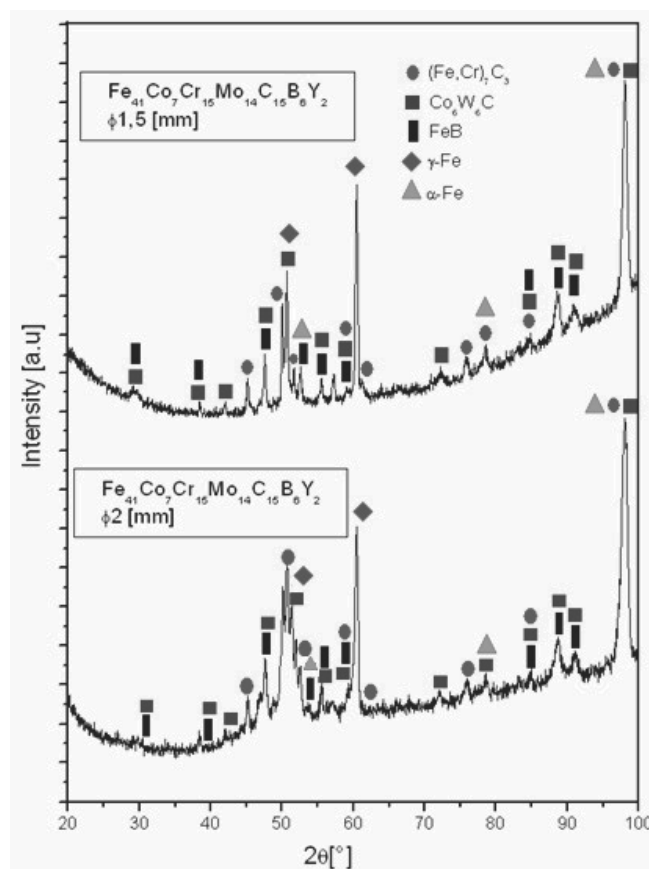


Fig. 2. X-ray diffraction patterns of the $\text{Fe}_{41}\text{Co}_7\text{Cr}_{15}\text{Mo}_{14}\text{C}_{15}\text{B}_6\text{Y}_2$ alloys rods with diameters of 1.5 mm and 2 mm

Fig. 3 presents the results of X-ray phase analysis for $\text{Fe}_{39}\text{Co}_7\text{Cr}_{15}\text{Mo}_{14}\text{C}_{15}\text{B}_6\text{Y}_4$ alloy. Based on the graphs it can be concluded that, as with previous samples, there is an increase of the background and the broadening of diffraction lines. This may indicate the creation of a small amount of amorphous phase.

Samples containing 2 at.% and 4 at.% of yttrium, with 1.5 mm and 2 mm diameter have similar phase composition. They differ from the composition of the sample containing no yttrium. There are the metallic phases (the same as those in the sample without yttrium) in those sample and similarly as the γ phase prevails, but the structure contained in these carbides is different. In both alloys the detected carbides are $(\text{Fe,Cr})_7\text{C}_3$ and $\text{Co}_6\text{W}_6\text{C}$. Taking in consideration the composition of the alloy samples is possible e.g. the actual pattern of the carbide $(\text{Fe,Cr})_6(\text{MoCr})_6\text{C}$ or approximate ones are possible. However the confirmation of this composition requires X-ray microanalysis study. Based on analyses there are found that there are probably the boride with structure of FeB and small amounts of other, unidentified crystalline phases. The presence of yttrium has not been found. It is probably only substituted by the part of atoms in the compounds of other metals, by changing their type of structure, but it does not form the compounds on their own.

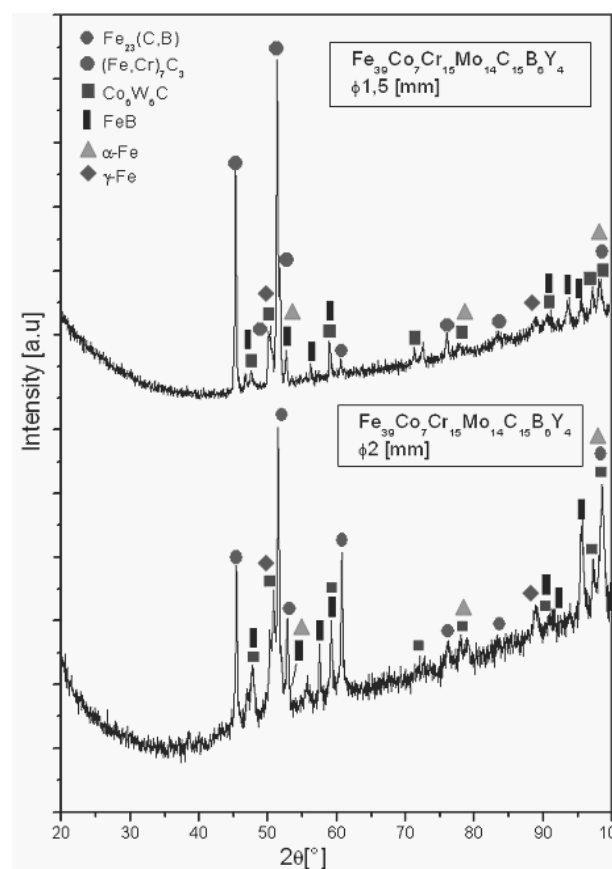


Fig. 3. X-ray diffraction patterns of the $\text{Fe}_{39}\text{Co}_7\text{Cr}_{15}\text{Mo}_{14}\text{C}_{15}\text{B}_6\text{Y}_4$ alloys rods with diameters of 1.5 mm and 2 mm

Alloys, which have in their composition yttrium, compared to samples of $\text{Fe}_{43}\text{Co}_7\text{Cr}_{15}\text{Mo}_{14}\text{C}_{15}\text{B}_6$ are characterized by bigger intensity of sharp crystalline peaks in relation to the sample of 2 at. % and 4 at. % yttrium. Alloying elements, which are part of

the obtained alloys exert a major impact not only on the properties of materials but also on their structure. The main addition of alloy which is most influential on the crystallization process and the structure is the yttrium. This process cause increase of the GFA but it also requires special and very precise conditions which accompany the process of casting. Moreover elements such as boron, chromium, and carbon have a major influence on both mechanical properties and structure of alloys.

The results of these studies might be influenced by many factors, primarily the specific chemical composition of the alloy, as well as cooling rate of alloys or parameters of the casting and melting process. Broadening and decreasing of the characteristic peaks for $\text{Fe}_{41}\text{Co}_7\text{Cr}_{15}\text{Mo}_{14}\text{C}_{15}\text{B}_6\text{Y}_2$ may indicate the creation of a small amount of amorphous phase.

3.2. The results of microscopic research

The fracture morphology and surface morphology of rods was investigated by scanning electron microscopy in different magnifications. Figs. 4-10 show samples of cast rods with diameters 1.5 mm and 2 mm.

Figs. 4 and 5 show the fracture morphology of the $\text{Fe}_{43}\text{Co}_7\text{Cr}_{15}\text{Mo}_{14}\text{C}_{15}\text{B}_6$ alloy rods with diameter 1.5 mm and 2 mm. The following figures 4 and 5 confirm crystalline structure $\text{Fe}_{43}\text{Co}_7\text{Cr}_{15}\text{Mo}_{14}\text{C}_{15}\text{B}_6$ alloy. Examination of fracture alloy with a diameter of 1.5 mm in the form of the rod (Fig. 4) shows that this fracture is characterized by morphology of brittle, intercrystalline, splintery fractures. In the figure the damage to the rod is also visible - a crack. It is cause by brittleness of the material.

Examination of the $\text{Fe}_{43}\text{Co}_7\text{Cr}_{15}\text{Mo}_{14}\text{C}_{15}\text{B}_6$ fracture alloy with a 2 mm diameter in the form of a rod showed that the alloy has a mixed structure. Fig. 5 shows similar morphology to the mixed fracture (ductile and brittle).

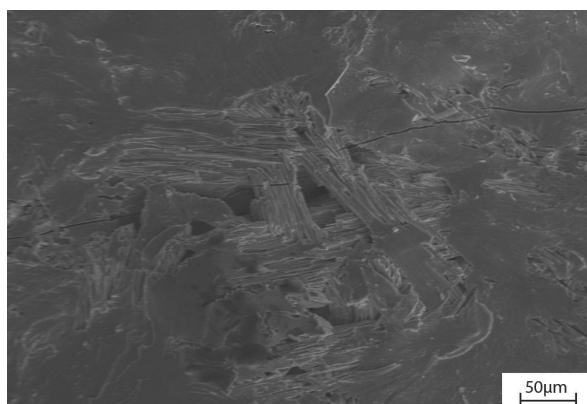


Fig. 4. SEM micrographs of the fracture morphology of $\text{Fe}_{43}\text{Co}_7\text{Cr}_{15}\text{Mo}_{14}\text{C}_{15}\text{B}_6$ rod in as - cast state with diameter of 1.5 mm (middle of sample)

The following rods show photo of obtained samples in the form of rods of the $\text{Fe}_{41}\text{Co}_7\text{Cr}_{15}\text{Mo}_{14}\text{C}_{15}\text{B}_6\text{Y}_2$ alloy with a 1.5 mm and 2 mm diameter (Figs. 6, 7, 8).

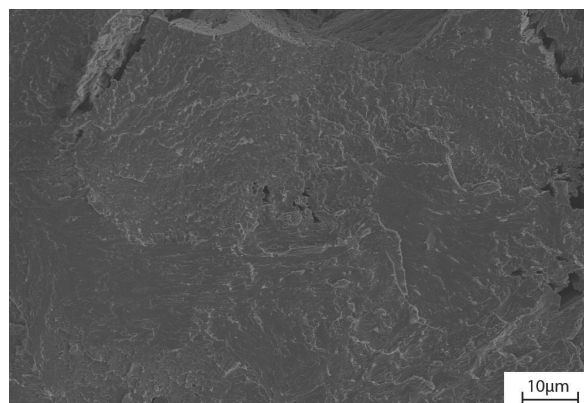


Fig. 5. SEM micrographs of the fracture morphology of $\text{Fe}_{43}\text{Co}_7\text{Cr}_{15}\text{Mo}_{14}\text{C}_{15}\text{B}_6$ rod in as - cast state with diameter of 2 mm (edge of sample)

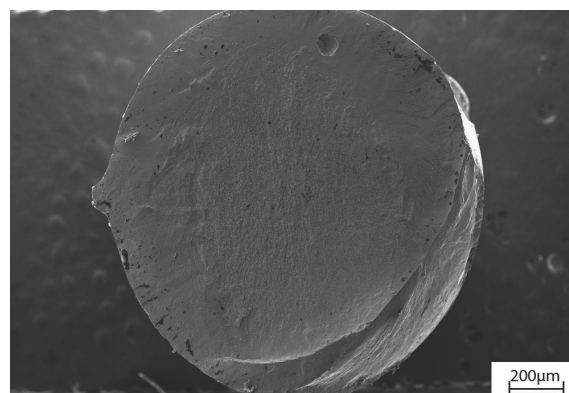


Fig. 6 SEM micrographs of the fracture morphology of $\text{Fe}_{41}\text{Co}_7\text{Cr}_{15}\text{Mo}_{14}\text{C}_{15}\text{B}_6\text{Y}_2$ rod in as - cast state with diameter of 1.5 mm (general view)

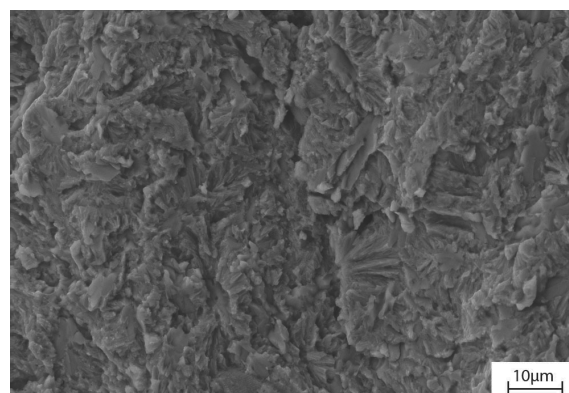


Fig. 7. SEM micrographs of the fracture morphology of $\text{Fe}_{41}\text{Co}_7\text{Cr}_{15}\text{Mo}_{14}\text{C}_{15}\text{B}_6\text{Y}_2$ rod in as - cast state with diameter of 1.5 mm

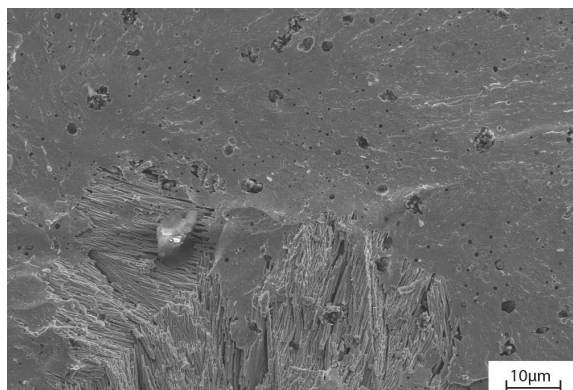


Fig. 8. SEM micrographs of the fracture morphology of $\text{Fe}_{41}\text{Co}_7\text{Cr}_{15}\text{Mo}_{14}\text{C}_{15}\text{B}_6\text{Y}_2$ rod in as - cast state with diameter of 2 mm (middle of sample)

Figs. 6 and 7 show $\text{Fe}_{41}\text{Co}_7\text{Cr}_{15}\text{Mo}_{14}\text{C}_{15}\text{B}_6\text{Y}_2$ alloy fracture with a 1.5 mm diameter. A lot of dendritic prime phase could be found. It is characteristic of alloys with crystalline structure. Non-uniform heat disposal during the solidification process of a substance causes that the crystal nucleus grow unevenly and grow faster in one direction, while in others more slowly. In such a case dendritic structure arises.

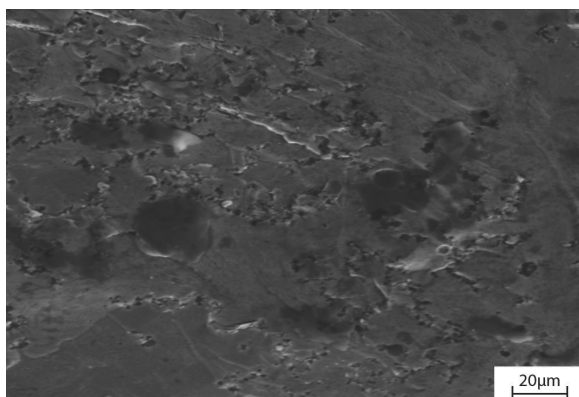


Fig. 9. SEM micrographs of the fracture morphology of $\text{Fe}_{39}\text{Co}_7\text{Cr}_{15}\text{Mo}_{14}\text{C}_{15}\text{B}_6\text{Y}_4$ rod in as - cast state with diameter of 1.5 mm (middle of sample)

Fig. 8 shows the morphology in the core of the rod of the $\text{Fe}_{41}\text{Co}_7\text{Cr}_{15}\text{Mo}_{14}\text{C}_{15}\text{B}_6\text{Y}_2$ alloy with diameter 2 mm. On the basis of examinations it was found that the sample has a visible "hole". In addition, there is the typical morphology for brittle and intercrystalline fracture. There are also visible surface irregularities.

Fig. 9 shows the microstructure of the rod of the $\text{Fe}_{39}\text{Co}_7\text{Cr}_{15}\text{Mo}_{14}\text{C}_{15}\text{B}_6\text{Y}_4$ alloy with diameter of 1.5 mm.

Figs. 9 and 10 which are from fracture of the sample show that the sample has a characteristic morphology for the mixed fracture with a small amount of brittle fracture. There are also visible surface irregularities.

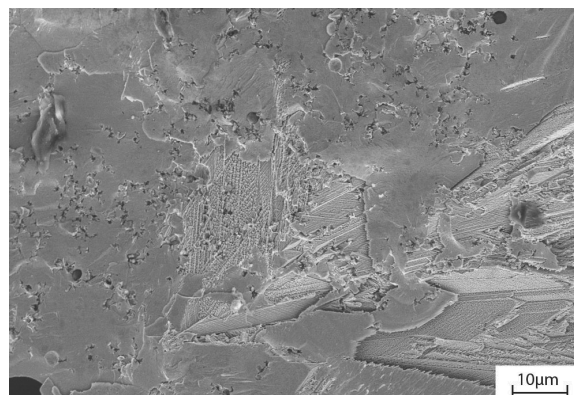


Fig. 10. SEM micrographs of the fracture morphology of $\text{Fe}_{39}\text{Co}_7\text{Cr}_{15}\text{Mo}_{14}\text{C}_{15}\text{B}_6\text{Y}_4$ rod in as - cast state with diameter of 1.5 mm (edge of sample)

Tests performed with using a scanning electron microscope showed that all of tested samples in a smaller or larger level are characterized by mixed structure. They also have small areas of smooth surface.

The $\text{Fe}_{43}\text{Co}_7\text{Cr}_{15}\text{Mo}_{14}\text{C}_{15}\text{B}_6$ alloy compared to alloys containing yttrium (2 at.% and 4 at.%) in their chemical composition is more brittle. The proof of this is the visible fracture on Fig. 4. The morphology of the fracture show that the alloy has also a smooth surface with some small amount of bulges. Although samples which contain in their chemical composition yttrium, have a similar to each other structure.

3.3. Results of the chemical composition

Chemical analysis was performed, using a distributed ray energy spectrometer EDS, which was equipped with a scanning electron microscope [21].

The analysis was performed on the surface of the fracture of the rod $\text{Fe}_{41}\text{Co}_7\text{Cr}_{15}\text{Mo}_{14}\text{C}_{15}\text{B}_6\text{Y}_2$ with 2 mm in diameter [21].

Based on the results of the chemical composition of the alloy, it has been confirmed the concentration of chemical elements [21].

3.4. Results of analysis of the crystallization process

The calorimetric curves were obtained through the study of thermal properties. These studies were designed to determine the thermal stability of the manufactured $\text{Fe}_{43}\text{Co}_7\text{Cr}_{15}\text{Mo}_{14}\text{C}_{15}\text{B}_6$, $\text{Fe}_{41}\text{Co}_7\text{Cr}_{15}\text{Mo}_{14}\text{C}_{15}\text{B}_6\text{Y}_2$ and $\text{Fe}_{39}\text{Co}_7\text{Cr}_{15}\text{Mo}_{14}\text{C}_{15}\text{B}_6\text{Y}_4$ alloys [21].

The main objective of this study was to determine the glass transition temperature and crystallization temperature [21].

On the thermograms cannot be identified a characteristic inflection of the measurement line. Calorimetric curves do not show structural changes that should occur in the test samples, under the influence of heat treatment. Despite the increase of temperature derivatograms do not change their position in the endothermic direction [21].

4. Conclusions

It is difficult to obtain a metallic glasses of $\text{Fe}_{43}\text{Co}_7\text{Cr}_{15}\text{Mo}_{14}\text{C}_{15}\text{B}_6$, $\text{Fe}_{41}\text{Co}_7\text{Cr}_{15}\text{Mo}_{14}\text{C}_{15}\text{B}_6\text{Y}_2$ and $\text{Fe}_{39}\text{Co}_7\text{Cr}_{15}\text{Mo}_{14}\text{C}_{15}\text{B}_6\text{Y}_4$ alloys. Taking into account all the factors affecting to the test samples, we can conclude that all operations designed to obtain amorphous structure were performed according to the following rules:

- the alloying elements had been weighed accurately,
- difference in atomic diameters is over 12%,
- the high purity of elements had been retained,
- the multicomponent alloy system consisting of more than tree elements had been chosen,
- the total melting of the initial feedstock had been found,
- negative heats of mixing among elements had been realised.

The metallic rods with diameter 1.5 mm and 2 mm were formed at $\text{Fe}_{43}\text{Co}_7\text{Cr}_{15}\text{Mo}_{14}\text{C}_{15}\text{B}_6$, $\text{Fe}_{41}\text{Co}_7\text{Cr}_{15}\text{Mo}_{14}\text{C}_{15}\text{B}_6\text{Y}_2$ and $\text{Fe}_{39}\text{Co}_7\text{Cr}_{15}\text{Mo}_{14}\text{C}_{15}\text{B}_6\text{Y}_4$ alloys by the pressure die casting method. The results obtained are summarized as follows:

- Based on the X-ray examinations it may be concluded that all tested alloys have crystalline structure. One can be concluded that alloys with yttrium addition are characterized by crystalline peaks which are less sharp than peaks for alloy without yttrium,
- Tests performed by using a morphology scanning electron microscope showed that the fracture of $\text{Fe}_{43}\text{Co}_7\text{Cr}_{15}\text{Mo}_{14}\text{C}_{15}\text{B}_6$, $\text{Fe}_{41}\text{Co}_7\text{Cr}_{15}\text{Mo}_{14}\text{C}_{15}\text{B}_6\text{Y}_2$ and $\text{Fe}_{39}\text{Co}_7\text{Cr}_{15}\text{Mo}_{14}\text{C}_{15}\text{B}_6\text{Y}_4$ alloys have a mixed structure, partly with a smooth surface. There are visible areas with small bulges surfaces. Microscopic observations showed that $\text{Fe}_{41}\text{Co}_7\text{Cr}_{15}\text{Mo}_{14}\text{C}_{15}\text{B}_6\text{Y}_2$ alloy has a lot of dendritic prime phase,
- The results of calorimetric research, represented by the calorimetric curves confirm that all of $\text{Fe}_{43}\text{Co}_7\text{Cr}_{15}\text{Mo}_{14}\text{C}_{15}\text{B}_6$, $\text{Fe}_{41}\text{Co}_7\text{Cr}_{15}\text{Mo}_{14}\text{C}_{15}\text{B}_6\text{Y}_2$ and $\text{Fe}_{39}\text{Co}_7\text{Cr}_{15}\text{Mo}_{14}\text{C}_{15}\text{B}_6\text{Y}_4$ rods with 1.5 mm and 2 mm in diameter are crystalline,
- The $\text{Fe}_{43}\text{Co}_7\text{Cr}_{15}\text{Mo}_{14}\text{C}_{15}\text{B}_6$ alloy as well as alloys containing 2 at.% Y and 4 at.% Y in their chemical composition show that the materials are brittle.

To obtain high GFA two aspect should be taken into consideration: stability of the liquid phase and resistance of the glassy phase to crystallization.

The lack of chemical heterogeneity control of obtained materials (ingots and rods) could be affected on the results of our research. There is necessity to the accurate uniform distribution of yttrium in materials.

References

- [1] W.H. Wang, Roles of minor additions in formation and properties of bulk metallic glasses, *Progress in Materials Science* 52 (2007) 540-596.
- [2] W.H. Wang, C. Dong, C.H. Shek, Bulk metallic glasses, *Materials Science and Engineering R* 44/2-3 (2004) 45-89.
- [3] E.S. Park, D.H. Kim, Phase separation and enhancement of plasticity in Cu-Zr-Al-Y bulk metallic glasses, *Acta Materialia* 54 (2006) 2597-2604.
- [4] J.M. Park, J.S. Park, J.H. Na, D.H. Kim, D.H. Kim, Effect of Y addition on thermal stability and the glass forming ability in Fe-Nb-B-Si bulk glassy alloy, *Materials Science and Engineering A* 435-436 (2006) 425-428.
- [5] S. Lesz, P. Kwapuliński, R. Nowosielski, Formation and physical properties of Fe-based bulk metallic glasses with Ni addition, *Journal of Achievements in Materials and Manufacturing Engineering* 31/1 (2008) 35-40.
- [6] W. Pilarczyk, R. Nowosielski, R. Babilas, A production attempt of selected metallic glasses with Fe and Ni matrix, *Archives of Materials Science and Engineering* 41/1 (2010) 5-12.
- [7] W. Pilarczyk, R. Nowosielski, A. Januszka, Structure and properties of Fe-Cr-Mo-C bulk metallic glasses obtained by die casting method, *Journal of Achievements in Materials and Manufacturing Engineering* 42 (2010) 81-87.
- [8] K. Amiya, A. Inoue, Fe-(Cr,Mo)-(C,B)-Tm bulk metallic glasses with high strength and high glass-forming ability, *Reviews on Advanced Materials Science* 18 (2008) 27-29.
- [9] Z.M. Wang, J. Zhang, X.C. Chang, W.L. Hou, J.Q. Wang, Susceptibility of minor alloying to corrosion behavior in yttrium-containing bulk amorphous steel, *Intermetallics* 16 (2008) 1036-1039.
- [10] X. Shan, H. Ha, J.H. Payer, Comparison of crevice corrosion of Fe-based amorphous metal and crystalline Ni-Cr-Mo alloy, *Metallurgical and Materials Transactions* 40 A (2009) 1324-1333.
- [11] Q. Chen, D. Zhang, Effect of hot isostatic pressing on mechanical properties of $\text{Fe}_{41}\text{Cr}_{15}\text{Mo}_{14}\text{C}_{15}\text{B}_6\text{Y}_2\text{Co}_7$ BMG, *International Journal of Modern Physics B* 20 (2006) 3617-3622.
- [12] S.F. Guo, Z.Y. Wu, L. Liu, Preparation and magnetic properties of FeCoHfMoBY bulk metallic glasses, *Journal of Alloys and Compounds* 468 (2009) 54-57.
- [13] C.Y. Lin, T.S. Chin, Soft magnetic (Fe, M)-Y-B (M=Co or Ni) bulk metallic glasses, *Journal of Alloys and Compounds* 437 (2007) 191-196.
- [14] X.H. Tan, H. Xu, Q. Bai, W.J. Zhao, Y.D. Dong, Magnetic properties of Fe-Co-Nd-Y-B magnet prepared by suction casting, *Journal of Non-Crystalline Solids* 353 (2007) 410-412.
- [15] H.W. Chang, Y.C. Huang, C.W. Chang, C.H. Chiu, W.C. Chang, Glass formability and soft magnetic properties of bulk Y-Fe-B-Ti metals, *Journal of Alloys and Compounds* 462 (2008) 68-72.
- [16] M. Regev, H. Rosenson, Z. Koren, A. Katz-Demyanetz, The influence of the cooling rate on bulk metallic glass formation in $\text{Mg}_{80}\text{Cu}_{15}\text{Y}_5$ and $\text{Mg}_{80}\text{Cu}_{10}\text{Y}_{10}$, *Journal of Materials Science* 45 (2010) 6365-6373.
- [17] J. Chen, Y. Zhang, J.P. He, K.F. Yao, B.C. Wei, G.L. Chen, Metallographic analysis of Cu-Zr-Al bulk amorphous alloys with yttrium addition, *Scripta Materialia* 54/7 (2006) 1351-1355.
- [18] S. Lesz, Z. Stokłosa, R. Nowosielski, Influence of copper addition on properties of $(\text{Fe}_{36}\text{Co}_{36}\text{B}_{19}\text{Si}_5\text{Nb}_4)_{100-x}\text{Cu}_x$ metallic glasses, *Archives of Materials Science and Engineering* 38/1 (2009) 12-18.
- [19] Z.M. Rdzawski, J. Stobrawa, W. Gluchowski, Structure and properties CuFe2 alloy, *Journal of Achievements in Materials and Manufacturing Engineering* 33/1 (2009) 7-18.
- [20] Jr. G. Johnson, V. Vand, To the powder diffraction file 1971, The Pennsylvania State University, Pennsylvania 1971.
- [21] A. Radko, The influence of yttrium addition on the structure and properties of Fe-Co-Cr-Mo-C-B-Y alloys, Silesian University of Technology Library, Gliwice, 2009 (in Polish).